

Impaired Response of Perforating Arteries to Hypercapnia in Chronic Hyperglycemia

XIMENA-SAYURI OIZUMI¹, TAICHI AKISAKI¹,
YOSHIYUKI KOUTA¹, XIU Z. SONG¹, TOSHIHIRO TAKATA¹,
TAKESHI KONDOH², KEIJI UMETANI³, MASATSUGU HIRANO³,
KATSUHITO YAMASAKI³, EIJI KOHMURA², KOICHI YOKONO¹
and TAKASHI SAKURAI¹

¹ Division of Internal and Geriatric Medicine, Kobe University Graduate School of Medicine

² Division of Neurosurgery, Kobe University Graduate School of Medicine

³ Japan Synchrotron Radiation Research Institute, SPring-8, Sayo-gun, Hyogo, Japan

Received 20 December 2005/ Accepted 20 January 2006

Key words: chronic hyperglycemia, hypercapnia, synchrotron radiation, cerebral vessels

Diabetes mellitus increases the risk of cerebrovascular disease, the effects of hypercapnia on CBF (cerebral blood flow) and cerebrovascular reactivity during diabetes are still inconsistent. Here, we have established a new microangiographic technique using synchrotron radiation (SPring-8, Japan), which enabled us to visualize rat cerebral vessels with high spatial resolution in real time. The goal of the study presented here was to identify the effects of chronic hyperglycemia on hypercapnia-induced vascular responses (endothelium-dependent vasodilatation) and nitric oxide (NO) donor-induced vascular responses (endothelium-independent) of perforating arteries and of the deeply located large cerebral arteries. We found a significant vasodilatation of rat perforating arteries after hypercapnia with a maximum diameter of approximately 140% of baseline in normal Wistar rats. Chronic hyperglycemia impaired vasodilatation of perforating arteries in genetically diabetic GK rats. SNP (sodium nitroprusside) caused a similar vasodilatation of perforating vessels in normal and chronic hyperglycemia, indicating that endothelium-dependent vasodilatation of perforating arteries may be specifically impaired in chronic hyperglycemia. Possible impairment of endothelium-dependent vasodilatation in perforating vessels during chronic hyperglycemia may cause decreased vascular reserve capacity of perforating artery, resulting in the increased ischemic insults and cerebrovascular diseases in diabetes.

Diabetes mellitus involves long-term vascular complications and hyperglycemia is recognized as the main cause in the pathogenesis of these diabetic vasculopathies. In brain, diabetes increases the risks of large and small cerebrovascular diseases and makes patients demonstrably more susceptible to cerebral ischemia (1). Hyperglycemia has been shown to increase neurologic deficits in models of hypoxic-ischemic-injury and it is possible that differences in the regulation of cerebral blood flow (CBF) could be responsible for this susceptibility (2).

Hypercapnia is a potent dilator of cerebral blood vessels, but the effects of hypercapnia on CBF and cerebrovascular reactivity during diabetes are still inconsistent. In human studies, impaired vascular responses to hypercapnia have been reported (3-5), while in animal

experiments it has been found that CBF responses to hypercapnia of cortical arterioles are comparable to normal animals (6-10).

Perforating arteries are terminal vessels directly emerging from the main cerebral arteries and particularly important because these arteries supply blood to brain structures such as basal ganglia, thalamus and hippocampus that are frequently impaired in diabetes (11). Distinctive branching pattern and higher intraluminal pressure of perforating artery may suggest the differential regulation of vascular reactivity from that of the pial arterioles. However, to our knowledge, there is not any report about the vascular response of perforating arteries *in vivo*. In this study, we used a newly developed microangiographic technique and investigated the vascular response to hypercapnia of rat perforating arteries. Therefore, the goal of the study presented here is to identify the effects of chronic hyperglycemia on hypercapnia-induced vascular responses (endothelium-dependent vasodilatation) and nitric oxide (NO) donor-induced vascular responses (endothelium-independent) of perforating arteries and of the deeply located large cerebral arteries.

METHODS

Experimental design and animal preparation

All experimental procedures were performed following the guidelines for animal experimentation at Kobe University Graduate School of Medicine. Six month-old Male Wistar-Kyoto and Goto-Kakizaki (GK) rats weighing 400 g - 450 g and 300 g - 350 g, respectively, were used. Animal rooms were controlled for temperature (23°C), humidity (55%) and light (12 h light-dark cycles).

In order to investigate the effects of hypercapnia on cerebral vascular reactivity, we divided the experimental animals into two groups. The first group comprised control Wistar rats (n=13). The second group comprised genetically diabetic GK rats (CLEA, Tokyo, Japan) (n=10). For the hypercapnic challenge rats inhaled CO₂ at 12% mixed in air for 5 min. Then rats were allowed to a 15 min period of recovery under normal capnia. To investigate the endothelium-independent vascular vasodilatation we applied sodium nitroprusside (SNP) (0.5 µg.kg⁻¹.min⁻¹, i.v.).

Microangiography and image analysis

Microangiographic imaging of the rat brain was performed at the third generation synchrotron radiation facility SPring-8 in Hyogo, Japan. The experimental arrangement for X-ray imaging using monochromatic synchrotron radiation X-rays at the SPring-8 BL20B2 beamline has been fully described elsewhere (12, 13) (Fig. 1). In brief, we used monochromatic synchrotron radiation as an X-ray source, which was obtained from an 8 GeV electron storage ring (Beamline BL20B2, SPring-8, Hyogo, Japan). X-Ray was monochromatized at 17 keV energy using a silicon double-crystal monochromator. The camera head incorporates an X-ray direct-sensing pick-up tube (Saticon). Absorbed X-rays in the photoconductive layer of the tube are directly converted into electron-hole pairs, and signal charges are read out by electron beam scanning. The digital images were acquired as 1024×1024 pixels with 10-bit resolution after analog-to-digital conversion. The field of view was 9.5 × 9.5 mm² and thus the pixel size was approximately 9.5 µm.

Under anesthesia (pentobarbital sodium, 50 mg/kg i.p.), rats were placed in the supine position in a stereotaxic frame with a window of 3 cm × 4 cm in the center of the platform for direct radiation of the head. After tracheotomy, each animal received pancuronium bromide (0.8 µmol/kg) and was mechanically ventilated with room air using a ventilator (SAR 830/P ventilator, California, U.S.A.) at a rate of 60-70 respirations/min. One femoral

PERFORATING ARTERIES DURING CHRONIC HYPERGLYCEMIA

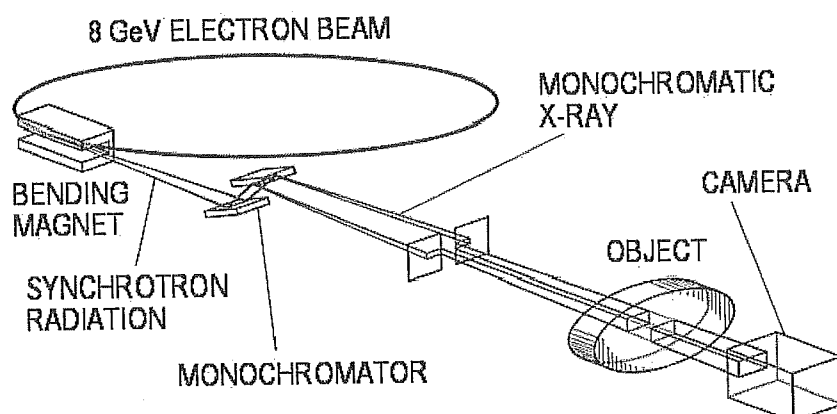


Figure 1 Illustration of the experimental arrangement at **BL20B2** beamline.

artery and one femoral vein were cannulated with PE-50 tubing (Natsume Manufacturing, Tokyo, Japan). The artery line was to measure systemic arterial blood pressure using a disposable pressure monitoring kit (Life Kit, Nihon Kohden, Tokyo, Japan) connected to a computer (Unique Acquisition, Unique Medical Company, Osaka, Japan). A femoral vein catheter was implanted for drug administration. Rectal temperature was maintained at 36-37°C with a heating pad. The right external carotid artery (ECA) was cannulated. The PE-50 tube inserted was connected to an automated injector (Auto Injector 120S, Nihon Kohden, Tokyo, Japan) that was programmed to reproducibly deliver 0.2 ml of nonionic contrast media (Iomeprol, Daiichi Pharmaceutical Company, Tokyo, Japan) in 0.4 second for each microangiographic imaging. For consistent measurement of the vascular diameters of these arteries, we established an exact measuring point for each vessel. For the measurement of the internal carotid artery (ICA), we chose a point at a distance of 665 μm from the posterior communicating artery (Pcom), for the medial cerebral artery (MCA), a point at a distance of 475 μm distant from the ICA bifurcation. Because perforating arteries have many anatomical variations in number and origin of the vessels (14), we selected the largest branches emerging from the MCA and determined a measuring point at 190 - 380 μm distant from the MCA for each of the perforating arteries. Measurements of vessel diameters after repetitive angiography were made consistently at the same point. On the stored digital images, vessel diameters were measured semi automatically with a software (Image-Pro Plus ver.4.0, Media Cybernetics Inc., Silver Spring, MD, USA) combined with a program developed for this study (15).

Experimental protocol

The first angiogram was recorded to estimate the baseline diameter of the vessels. Hypercapnia was induced by inhalation of CO₂ at 12% mixed in air for 5min. The arterial blood gas were analyzed, and the inhalation was returned to normal room air. An additional angiograph was made at 15 min under normocapnia and arterial blood gases were analyzed. On separate experiments, an infusion pump was connected to the vein catheter and SNP was injected continuously at a flow rate of 0.4 ml/min

Measurements of blood gases and glucose

Arterial blood gas tensions and pH were measured with an i-STAT G3 + Cartridge (Abbott Point-of-Care, East Windsor, NJ, USA) and blood glucose concentrations were measured by a Glutest-S analyzer (Shiga, Japan).

Statistical analysis

Values are expressed as mean ± standard error. One way analysis of variance (ANOVA) was used for the comparison of more than two groups. Post-hoc comparisons between mean values were made with Scheffe's test. P value < 0.05 was accepted as statistically significant.

RESULTS

Table 1 shows the effects of CO₂ inhalation on the average pH, PaO₂, PaCO₂ of arterial blood gas from control and GK rats. We determined the initial diameter of each vessel before induction of hypercapnia, there was no statistical difference between the two groups. Baseline diameter for ICA was 232±17.8 μm and 278±45.2 μm, in Wistar and GK rats, respectively. For MCA, 211.4 μm±9.9 and 190.0±8.2 μm in Wistar and GK rats, respectively. For perforating arteries, baseline diameters were 77.1±4.6 μm and 91.5±9.8 μm in Wistar and GK rats, respectively. Figure 2 represents the response of perforating arteries to hypercapnia in control rats at baseline (Fig. 2A) and after 5 min of CO₂ administration (Fig. 2B).

Table 1. Arterial Blood Values

	WISTAR				GK			
	CO ₂	O ₂	pH	BS(mM)	CO ₂	O ₂	pH	BS(mM)
0 min.	30.9±4.1	107.1±5.6	7.5±0.1	6.5±0.5	33.3±2.7	101.8±6.5	7.4±0.1	15.2±1.4 *
5 min.	86.9±9.7	101.7±3.0	7.1±0.4	-	101.0±6.5	108.2±2.9	7.0±0.1	-
R15 min.	33.8±7.1	113.5±8.3	7.3±0.8	-	27.0±1.0	96±20.0	7.7±0.1	-

BS, blood sugar. 0 min, baseline. 5 min, after CO₂ administration. R15, room air. Data are Mean±S.E. *P < 0.01 vs. control

Figure 2

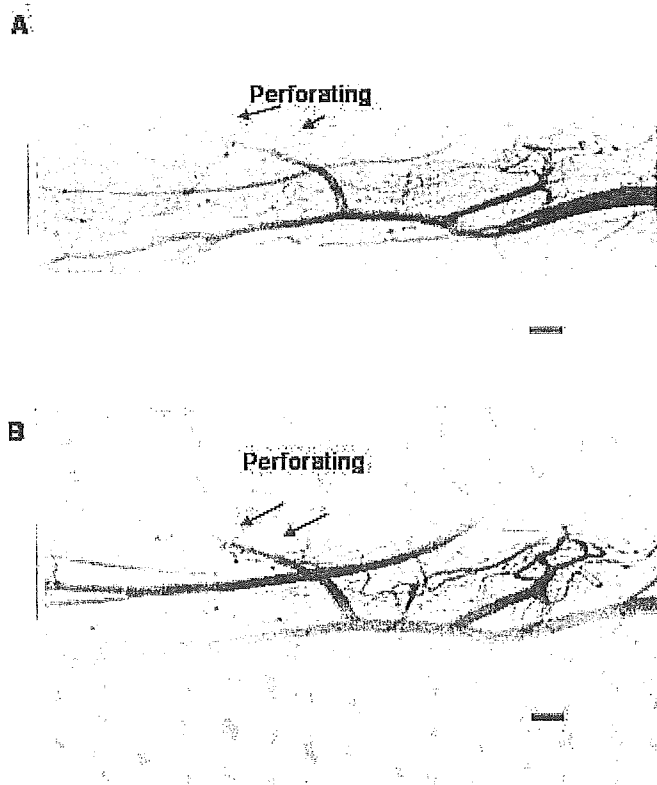


Figure 2

Photographs of perforating arteries emerging from the MCA (arrows) at rest (A), and during hypercapnia (B). Diameters of perforating vessels in this example were 80.5 μm at rest and 116.15 μm during hypercapnia respectively. Scale bar=300 μm.

PERFORATING ARTERIES DURING CHRONIC HYPERGLYCEMIA

Table 2 shows the steady-state responses to hypercapnia of the diameters in ICA, MCA and perforating vessels of normal Wistar and GK rats. In ICA and MCA we found a significant increase of diameter after 5 min hypercapnia for Wistar rat (126% and 142% of baseline diameter, respectively), GK rat also tended to show vasodilatation but failed to be significant. The vessel diameter returned to baseline value after the CO₂ challenge (Table 2). Perforating vessels showed significant vasodilatation to hypercapnia in the control group (135%), but in the GK group, vasodilatation was observed at insignificant rate (112%). The vessel diameter returned to baseline value after the CO₂ challenge (Table 2).

Table 2. Effect of hypercapnia on cerebral blood vessels

	Wistar			GK		
	ICA	MCA	PERF	ICA	MCA	PERF
0 min.	100	100	100	100	100	100
5 min.	126±6.8*	142±11.0*	135±11.3*	117±18.3	114±7.7	112±17.3
R15 min.	99±8.3	100±11	106±9.5	82±3.5	101±14.5	98±8.0

Values are means ± SE in % of change of baseline diameter.

5 min., CO₂ inhalation. R15, room air 15 mins. *P < 0.01 from 0 min

Nitric Oxide donor, SNP, caused a significant vasodilatation of perforating arteries of both, control and GK groups (126% and 120%, respectively) (Table 3). ICA and MCA arteries did not show any significant changes (Table 3).

Table 3. Effect of SNP on cerebral blood vessels

	Wistar			GK		
	ICA	MCA	PERF	ICA	MCA	PERF
0 min.	100	100	100	100	100	100
10 min.	101±2.3	103±2.7	126±3.9**	105±4.0	110±3.0	120±7.8+

Values are means ± SE in % change of baseline diameter

10 min., 10 min. infusion of SNP. **P < 0.001 from 0 min. +P < 0.01 from 0 min.

DISCUSSION

This study is the first to directly investigate the effects of diabetes on the response of perforating arteries to hypercapnia and NO donor. We found a significant vasodilatation of rat perforating arteries with a maximum diameter of approximately 140% of baseline in normal Wistar rats after hypercapnia. In contrast, chronic hyperglycemia impaired vasodilatation of perforating arteries in genetically diabetic GK rats. Secondly, SNP caused a similar vasodilatation of perforating vessels in normal and diabetic rats, indicating that endothelium-dependent vasodilatation of perforating arteries may be specifically impaired in chronic hyperglycemia.

Previous experiments have revealed an intact CO₂ response of cerebral cortical arterioles in the diabetic dogs and STZ-induced diabetic rats (6, 8, 16). In contrast, human studies have (3-5) revealed that diabetic patients failed to respond normally to hypercapnia. Kadoi et al also suggested that the impaired response was related to severity of diabetes mellitus (5). The interpretation of clinical studies is complicated by the association of diabetes with microangiopathy and large vessel diseases. Therefore, we investigated the morphological changes in cerebral arteries in brains from 6-month and 12-month-old GK rats prior to this angiographic experiment. It has been reported that diabetes produces thickening of the

arterial wall, perivascular and interstitial fibrosis, microaneurysms, arteriolar hyalinosis, and atheromatosis (17-19), which could account for the pathogenesis of diabetic cerebrovascular disorders. In 6-month-old GK rats, however, cerebral arteries, including the MCA and perforating vessels did not show such microscopic alterations, nor could we find any significant microscopic changes in the of 12-month-old GK rats (data not shown). Thus, we think that the impaired reactivity to hypercapnia of deeply located vessels including perforating arteries could be due to hyperglycemia, rather than diabetic microangiopathy in GK brains.

In another set of experiments, we have analyzed the effects of hyperglycemia on the blood pressure induced vascular dilatation (autoregulation) of perforating arteries. We have found that autoregulatory responses were reversibly impaired in GK rats (data not shown), which supported the notion that perforating arteries of GK rats had functional loss of endothelium-dependent vasodilatation, rather than structural deficits of cerebral blood vessels. The discrepancy between previous findings and our findings may be related to the difference of animal models and/or the experimental technique such as anesthesia that could affect the vascular responses. Regional differences in the response of cerebral blood vessels have been specially noted in previous experiments (20).

Several mechanisms have been proposed for the hypercapnia induced cerebrovascular vasodilatation. Hypercapnia requires the development of extracellular acidosis (21-23). NO is a major mediator of endothelium-dependent relaxation in various vascular beds, and plays an essential role in regulation of the cerebral circulation. Iadecola et al. demonstrated that nitric oxide synthase (NOS) inhibitors attenuated the CBF response to hypercapnia that occurs only at $\text{PaCO}_2 < 100$ mmHg (24). You et al. suggested that the cerebral vasorelaxation elicited by CO_2 was not related with an increase in NOS activity (22). This might indicate that the cerebral vasodilatation elicited by hypercapnia has NO-dependent and NO-independent components. It is likely that NO plays a role in the response to hypercapnic acidosis and it is partly responsible for the increase of cerebral blood flow during hypercapnia (23, 25, 26). There is enough evidence of the existence of ATP-sensitive potassium channels (K_{ATP}) in cerebral blood vessels, and therefore their implication in the vasodilatation of cerebral arteries to hypercapnia has also been investigated. Faraci et al. found that glibenclamide attenuated the dilatation of cerebral arterioles in response to a low concentration of acetylcholine and moderate hypercapnia (27).

In diabetes, functional impairment of NO and K_{ATP} channels-mediated vasodilatation have been suggested of pial arterioles and the basilar artery (28-29). Diabetes is associated with an increased generation of oxygen-derived free radicals in vascular tissues, and reactive oxygen species could influence the structure and activity of K_{ATP} channels (19, 29-32). Continuous production of reactive oxygen species produces an impaired vascular response of perforating arteries during chronic hyperglycemia.

There is considerable controversy regarding the effects of NO donors on vascular reactivity. It has been reported that application of intracarotid SNP fails to augment CBF (33, 34), and that the degree of vasodilatation varies in iliac and superior mesenteric arteries (35). The discrepancy between experiments seems to be inconsistent across animal species and vascular bed examined. However, we could find that application of SNP increased the vascular diameter similarly in control and diabetic rats, suggesting that impaired vasodilatation of perforating arteries to hypercapnia is due to the deficit in NO production/release in vascular endothelium in part during chronic hyperglycemia.

In summary, we could demonstrate the *in vivo* evidences for the first time that responses of rat perforating arteries to hypercapnia are specifically disrupted during diabetes mellitus.

PERFORATING ARTERIES DURING CHRONIC HYPERGLYCEMIA

Possible impairment of endothelium-dependent vasodilatation in perforating vessels during chronic hyperglycemia may cause decreased vascular reserve capacity of perforating artery, resulting in the increased ischemic insults and cerebrovascular diseases in diabetes. Further studies are needed to know the cellular mechanism of hyperglycemic impacts on cerebrovascular reactivity.

ACKNOWLEDGEMENTS

We deeply appreciate Dr. Haruo Yamashita, Dr. Bo Yang, Dr. Yoshikazu Ryu, Dr. Takuya Teranishi, Dr. Abesh K. Bhattacharjee, Dr. Seiji Nakajima, Dr. Akitsugu Morishita, Dr. Masahiro Tamaki, Dr. Takashi Mizobe, Dr. Junji Koyama, Dr. Kazuhiro Tanaka and Dr. Keiji Kidoguchi for their technical assistance. This work was supported by a Research Grant from the Novartis Foundation for Gerontological Research and a Grant-in-Aid for Scientific Research (17500473) from Japan Society for the Promotion of Science (T.S.). Synchrotron radiation experiments were performed at the SPring-8 BL20B2 beamline with the approval of the Japan Synchrotron Radiation Research Institute (Acceptance Nos. 2002A0079-NL2-np, 2002B0312-NL2-np, and 2004A0313-NL3-np).

REFERENCES

1. **Karapanayiotides T, Piechowski-Jozwiak B, van Melle G, Bogousslavsky J, Devuyst G.** 2004. Stroke patterns, etiology, and prognosis in patients with diabetes mellitus. *Neurology* **11**; 62(9): 1558-62.
2. **LeBlanc MH, Huang M, Vig V, Patel D, Smith EE.** 1993. Glucose affects the severity of hypoxic-ischemic brain injury in newborn pigs. *Stroke* **24**(7): 1055-62.
3. **Dandona P, James IM, Newbury PA, Woollard ML, Beckett AG.** 1978. Cerebral blood flow in diabetes mellitus: evidence of abnormal cerebrovascular reactivity. *Br Med J.* **2**(6133): 325-6.
4. **Griffith DN, Saimbi S, Lewis C, Tolfree S, Betteridge DJ.** 1987. Abnormal cerebrovascular carbon dioxide reactivity in people with diabetes. *Diabet Med.*, **4**(3): 217-220.
5. **Kadoi Y, Hinohara H, Kunimoto F, Saito S, Ide M, Hiraoka H, Kawahara F, Goto F.** 2003. Diabetic patients have an impaired cerebral vasodilatory response to hypercapnia under propofol anesthesia. *Stroke* **34**: 2399-2403.
6. **Simpson RE, Phillis JW, Buchannan J.** 1990. A comparison of cerebral blood flow during basal, hypotensive, hypoxic and hypercapnic conditions between normal and streptozotocin diabetic rats. *Brain Research*, **531**: 136-142.
7. **Cenic A, Craen RA, Howard-Lech VL, Lee TY, Gelb AW.** 2000. Cerebral blood volume and blood flow at varying arterial carbon dioxide tension levels in rabbits during propofol anesthesia. *Anesth Analg*, **90**: 1376-1386.
8. **Sieber FE, Brown PR, Wu Y, Koehler RC, Traystman RJ.** 1993. Cerebral blood flow responsiveness to CO₂ in anesthetized chronically diabetic dogs. *Am J Physiol.* **264**: H1069-H1075.
9. **Kawata R, Nakakimura K, Matsumoto M, Kawai K, Kunihiro M, Sakabe T.** 1998. Cerebrovascular CO₂ reactivity during anesthesia in patients with diabetes mellitus and peripheral vascular disease. *Anesthesiology* **89**(4): 887-893.
10. **Rodriguez G, Nobili F, Celestino MA, Francione S, Gulli G, Hassan K, Marengo S, Rosadini G, Cordera R.** 1993. Regional cerebral blood flow and cerebrovascular reactivity in IDDM. *Diabetes Care* **16**(2): 462-468.

11. **Groot J, Leeuw FE, Oudkerk M, van Gijn J, Hofman A, Jolles J, Breteler M.** 2000. Cerebral white matter lesions and cognitive function: the Rotterdam Scan Study. *Ann Neurol.* **47**: 145-151.
12. **SPring-8.** 2000. Medical and Imaging I (BL20B2). SPring-8 Annual Report. **1999**: 54-55.
13. **Umetani K, Yamashita T, Maehara N, Tokiya R, Imai S, Kajihara Y.** 2003. Small-field angiographic imaging of tumor blood vessels in rabbit auricle using X-ray SATICON camera and synchrotron radiation. Proc. 25th Annual Int. Conf. of the IEEE Engineering in Medicine and Biology Society. Cancún 978-981.
14. **Rieke GK, Bowers DE, Penn P.** 1981. Vascular supply pattern to rat caudatoputamen and globus pallidus. Scanning electronmicroscopic study of vascular endocasts of stroke-prone vessels. *Stroke* **12**: 840-846.
15. **Hirano M, Yamasaki K, Sakurai T, Kondoh T, Ryu Y, Okada H, Sugimura K, Kitazawa S, Kitazawa R, Maeda S, Katafuchi T, Tamura S.** 2003. Measurement of blood vessel diameter for angiography using refraction contrast imaging. *Igaku Butsuri*: **23**:157-159.
16. **Wang Q, Pelligrino DA, Koenig HM, Albrecht RF.** 1994. The role of endothelium and nitric oxide in rat pial arteriolar dilatory responses to CO₂ in vivo. *J Cereb Blood Flow Metab*,
17. **Muruganandan S, Srinivasan K, Gupta S, Gupta PK, Lal J.** 2005. Effect of mangiferin on hyperglycemia and atherogenicity in streptozotocin diabetic rats. *J Ethnopharmacol* **97(3)**:497-501.
18. **Velasquez MT, Kimmel PL, Michaelis OE 4th.** 1990. Animal models of spontaneous diabetic kidney disease. *FASEB J.* **4**: 2850-2859.
19. **Yu Y, Ohmori K, Kondo I, Yao L, Noma T, Tsuji T, Mizushige K, Kohno M.** 2002. Correlation of functional and structural alterations of the coronary arterioles during development of type II diabetes mellitus in rats. *Cardiovascular Research* **56**: 303-311.
20. **Duckrow R, Beard D, Brennan R.** 1987. Regional cerebral blood flow decreases during chronic and acute hyperglycemia. *Stroke* **18**: 52-58.
21. **Kontos HA, Wei EP, Raper AJ, Patterson JL.** 1977. Local mechanism of CO₂ action on cat pial arterioles. *Stroke* **8**:226-229.
22. **You JP, Wang Q, Zhang W, Jansen-Olesen I, Paulson OB, Lassen NA, Edvinsson L.** 1994. Hypercapnic vasodilatation in isolated rat basilar arteries is exerted via low pH and does not involve nitric oxide synthase stimulation or cyclic GMP production. *Acta Physiol Scand* **152**: 391-397.
23. **Tian R, Vogel P, Lassen NA, Mulvany MJ, Andreassen F, Aalkjaer C.** 1995. Role of extracellular and intracellular acidosis for hypercapnia-induced inhibition of tension of isolated rat cerebral arterioles. *Circ Res* **76**: 269-275.
24. **Iadecola C, Zhang F.** 1994. Nitric oxide-dependent and -independent components of cerebrovasodilatation elicited by hypercapnia. *Am. J. Physiol.* **266**: R546-R552
25. **Iadecola C.** 1992. Does nitric oxide mediate the increases in cerebral blood flow elicited by hypercapnia?. *Proc. Natl. Acad. Sci.* **89**: 3913-3916.
26. **Wang Q, Palson OB, Lassen NA.** 1992. Effect of nitric oxide blockade by NG-nitro-L-arginine on cerebral blood flow response to changes in carbon dioxide tension. *J. Cereb. Blood Flow Metab.* **12**: 935-946.
27. **Faraci FM, Breese KR, Heistad DD.** 1994. Cerebral vasodilatation during hypercapnia. Role of glibenclamide-sensitive potassium channels and nitric oxide. 1994. *Stroke* **25**: 1679-1683.

PERFORATING ARTERIES DURING CHRONIC HYPERGLYCEMIA

28. **Mayhan W, Faraci F.** 1993. Responses of cerebral arterioles in diabetic rats to activation of ATP-sensitive potassium channels. *Am. J. Physiol. (Heart Circ. Physiol.* **34**): H152-157.
29. **Matsumoto T, Yoshiyama S, Wakabayashi K, Kobayashi T, Kamata K.** 2004. Effect of chronic insulin on cromakalim-induced relaxation in established streptozotocin-diabetic rat basilar artery. *Eur. J. Pharmac.* **504**: 129-137
30. **Faraci FM, Heistad DD.** 1998. Regulation of the cerebral circulation: role of endothelium and potassium channels. *Physiol Rev.* **78**: 53-97.
31. **Niedowicz DM, Daleke DL.** 2005. The role of oxidative stress in diabetic complications. *Cell Biochem Biophys.* **43**: 289-330.
32. **Erdoş B, Simandle SA, Snipes JA, Miller AW, Busija DW.** 2004. Potassium channel dysfunction in cerebral arteries of insulin-resistant rats is mediated by reactive oxygen species. *Stroke* **35**: 964-9.
33. **Young WL, Prohovnik I, Schroeder T.** 1990. Intraoperative ¹³³Xe cerebral blood flow measurements by intravenous versus intracarotid methods. *Anesthesiology* **73**: 637-643.
34. **Joshi S, Duong H, Mangla S, Wang M, Libow AD, Popilskis S, Ostapkovich ND, Wang TS, Young WL, Pile-Spellman J.** 2002. In nonhuman primates intracarotid adenosine, but not sodium nitroprusside, increases cerebral blood flow. *Anesth Analg* **94**: 393-399.
35. **Martinez-Nieves B, Dunbar JC.** 1999. Vascular dilatatory responses to sodium nitroprusside (SNP) and α -adrenergic antagonism in female and male normal and diabetic rats. *P.S.E.B.M.* **222**: 90-98.

Neuroprotective Effect of D-Fructose-1,6-Bisphosphate against β -Amyloid Induced Neurotoxicity in Rat Hippocampal Organotypic Slice Culture: Involvement of PLC and MEK/ERK Signaling Pathways

XIUZHEN SONG¹, BIN WU², TOSHIHIRO TAKATA¹,
XIAONAN WANG¹, XIMENA-SAYURI OIZUMI¹, TAICHI AKISAKI¹,
KOICHI YOKONO¹, and TAKASHI SAKURAI¹

¹ *Division of Internal and Geriatric Medicine, Kobe University Graduate School of Medicine*

² *Open Research Center of Lifestyle-Related Diseases, Mukogawa-Women's University,
Nishinomiya, Japan*

Received 24 November 2005 /Accepted 6 January 2006

Key Words: Alzheimer's disease; D-fructose-1,6-bisphosphate; Amyloid Beta-peptide; Adenosine triphosphate; Phospholipase C; Mitogen activated extracellular signal protein kinase; Extracellular signal activated protein kinase

D-fructose-1,6-bisphosphate (FBP) is an endogenous intermediate of glycolytic pathway which has potent neuroprotective effect against various neurotoxic insults. This study examined whether FBP could antagonize the neurotoxicity induced by amyloid β -peptide (A β) in rat hippocampal organotypic slice cultures, and the possible mechanism was also explored. Treatment with FBP (concentration ranges from 1.7 mM to 10 mM) significantly decreased the cell death in hippocampal slices in the presence of A β at 24h, 48h and 72h, and this neuroprotective effect of FBP against A β was not in a dose-dependent manner, FBP 3.5 mM has better neuroprotective effect than that of other FBP concentration groups. Treatment with FBP slightly but significantly increases the ATP levels in hippocampal slices in the presence of A β . However, the increment of ATP levels was similar among various FBP concentration groups. Neuroprotective effect of FBP 3.5 mM against A β induced neurotoxicity in hippocampal slices was attenuated by addition of phospholipase C (PLC) inhibitor, U73122, mitogen activated extracellular signal protein kinase (MEK) inhibitor, U0126, or extracellular signal activated protein kinase (ERK) inhibitor, PD98059 at 24h, 48h and 72h. However, co-treatment with these three kinds of inhibitors did not change the FBP's effect on ATP levels. Our results suggested FBP has neuroprotective effect against A β induced neurotoxicity in hippocampal slice cultures, and FBP plays role not only as an alternative energy source, but also a modulator of PLC and MEK/ERK pathways to regulate the cellular response and survival.

Alzheimer's disease (AD) is a progressive senile dementia characterized by deposition of A β in the form of senile plaques and the microtubule associated protein tau as paired helical filaments. A β is a 4 kDa peptide of 39-42 residues which has multi neurotoxic effects leading to the dysfunction and death of neurons (33). Both in vitro and in vivo studies have confirmed the crucial role of A β in the development of AD. Progressive neuronal loss in AD is considered to be a consequence of the neurotoxic properties of A β (14). From this point of

view, preventing the A β induced neurotoxicity is of great importance for the development of potent therapeutic strategies.

D-fructose-1,6-bisphosphate (FBP), an endogenous intermediate of glycolytic pathway, can protect organ system from lethal injury accompanying ischemia or shock (21). There is some other evidence that FBP attenuates brain damage induced by hypoxia-ischemia (15), insulin induced hypoglycemia (7) and cardiogenic shock (34). FBP is also reported to provide protection of neurons against stimulated ischemia in hippocampal slices (19). The mechanisms by which FBP protects the brain neurons are not well understood. Possible mechanisms of protection include anaerobic metabolism of FBP to yield ATP (9) or its ability to reduce ATP loss (11), calcium chelation (13) and modulation of second messenger system.

Up to date, whether the neurotoxicity of A β in hippocampus could be antagonized by FBP is not well documented. We conducted this study to examine if FBP has the neuroprotective effect against A β induced toxicity using organic hippocampal slices. Furthermore, to determine whether FBP serves as an alternative energy sources to preserve neuronal survival, we examined the effects of exogenous FBP on ATP levels in organic hippocampal slices during A β neurotoxication. Recently many studies also indicate that FBP exerts its neuroprotective effect by modulating intracellular signaling pathways. A few intracellular signaling pathways, such as PLC and MEK/ERK (6) are reported to be associated with the neuroprotective effects of FBP, and thus we investigated here if these pathways are involved in the effects of FBP on the A β induced neurotoxicity.

MATERIALS AND METHODS

The experiments were conducted according to the guidelines for animal experimentation at the Kobe University School of Medicine and conform to relevant National Institution of Health guidelines.

Preparation of organotypic hippocampal slices

Hippocampal slices were made from the septal half of the hippocampus using a standard method (28). Briefly, 9-11 days Wistar rats (Hartley, SLC, Japan) were anesthetized with 98% Diethyl Ether and decapitated. The hippocampi were rapidly dissected at 4-6°C and cut into 450 μ m slices using a McIlwain Tissue Chopper (Mickle Laboratory Engineering Co.Ltd, UK). Slices were then transferred onto 30- μ m diameter-pored membrane (Millicell-CM, Millipore, Bedford, MA, USA), and put into a six-well microplate (Costar Corning Inc, NY, USA) with 1ml slice culture media per well. The culture media contained 50% Eagles minimal essential medium (MEM) (Gibco, CA, USA), 25% Hanks' Balanced Salt Solution (HBSS) (Gibco, CA, USA), 25% heat inactivated horse serum (Gibco, CA, USA) containing 1% penicillin/streptomycin. Slices were kept in culture for 14 days before study and the six-well micropaltes were stored at 37°C in a 95% humidified atmosphere with 5% CO₂ incubator (Sanyo, Tokyo, Japan).

Treatment of hippocampal slices

Slices in six-well micropaltes at day 14 were washed, and the basic medium was replaced with various agents for the treatment. The basic medium contained 90mM NaCl, 4mM KCl, 0.1mM MgCl₂, 0.1mM KH₂PO₄, 0.5 mM MgSO₄, 0.1 mM Na₂HPO₄, 0.5 mM NaH₂PO₄, 14 mM NaHCO₃, 1.2 mM CaCl₂, 10 mM glucose, about 2 mM essential and non-essential amino acids, 0.02 mM vitamins. To establish the A β induced neurotoxicity, slices were treated with three kinds of A β peptides (A β ₂₅₋₃₅, A β ₁₋₄₀, and A β ₁₋₄₂) in various concentrations. A β ₂₅₋₃₅, A β ₁₋₄₀, and A β ₁₋₄₂ (Peptide Institute Inc. Japan, Osaka) were dissolved in sterilized distill water. To assure full contact between A β and the culture,

NEUROPROTECTIVE EFFECTS OF FBP AGAINST A β

treatment media was applied from underneath the insert onto the culture by pipetting at first 4h. Various concentrations of FBP (Sigma, St. Louis, MO, USA) were added to the culture with or without A β_{25-35} for determining the FBP's effect against the A β induced neurotoxicity. To determine whether a signaling pathway is involved in the neuroprotective effect of FBP, a few signaling pathway-specific inhibitors were used, including a phospholipase-C (PLC) inhibitor, U73122 (Wako, Osaka, Japan), a mitogen activated extracellular signal protein kinase (MEK1/2) inhibitor, U0126 (Wako, Osaka, Japan), an extracellular signal activated protein kinase (ERK) inhibitor, PD98059 (Wako, Osaka, Japan), and a protein kinaseC (PKC) inhibitor, chelerythrine (Calbiochem Merck, Tokyo, Japan). Each pathway-specific inhibitors (10 μ M) was added into the slice culture with or without various concentrations of FBP and A β_{25-35} .

Assessment of cell death in hippocampal slices

Propidium iodide (PI) method was applied for the assessment of neuron death in hippocampal slices at 24h, 48h, and 72h after each treatment in the CA1 region of the hippocampus. To label the nuclei of dead neurons, 4.6 μ g/ml PI (Sigma, Louis.St, Mo, USA) was added to the wells of the culture microplates for 15 min. PI is a polar compound which only enters cells with damaged cell membranes. Inside the cells it binds to nucleic acids and becomes brightly red fluorescent. The dye is basically non-toxic to neurons and has been used as an indicator of neuronal integrity and cell viability (20). Thus the intensity of fluorescence is parallel to the cell death. After 15 min, digital images of PI fluorescence were obtained with an inverted fluorescence microscope (4 \times objective) equipped with a digital camera (Olympus IX70, Tokyo, Japan). After the final image, all the neurons were killed by adding 10 μ M N-Methyl-D-Aspartic Acid (NMDA) and the final PI fluorescence intensity was adjusted equivalent to 100% cell death. The mean intensity (green values) of the PI fluorescence were measured using an image program MacScope (Ver 2.6.1, Mitani Inc, Osaka, Japan).

Measurement of ATP levels

Hippocampal slices were dissected under a microscope at 48h after each treatment. Four slices were immediately homogenized in 0.5 N perchloric acid with 1 mM thylene-diaminetetra acetic acid and centrifuged for 15min at 2000rpm. The supernatant was neutralized with 2M KHCO₃, recentrifuged and stored at -30°C until assay of ATP. ATP was quantitated enzymatically and fluorometrically by measuring the production of nicotinamide adenine dinucleotide phosphate hydride (29). Protein content of the slices was determined by the method of Lowry and Passonneau (25).

Statistical analysis

Data was expressed as mean \pm standard error of the mean (s.e.m) from three independent experiments. Statistical significance was established by ANOVA followed by post-hoc test using SPSS (Ver 12.0, SPSS, Inc., Chicago, USA) software. $P < 0.05$ was considered to be statistically significant.

RESULTS

Neurotoxicity of A β

Three different kinds of A β fragments, A β_{25-35} , A β_{1-40} , and A β_{1-42} , were applied to establish the neurotoxicity of A β . Cell death was evaluated at 48h after various concentrations of three A β fragments administration. A β_{1-40} , and A β_{1-42} caused up to 40%-70% cell death at concentrations ranging from 0.5 μ M to 50 μ M. A β_{25-35} (50 μ M) induced similar toxicity comparable to A β_{1-40} , and A β_{1-42} at 25 μ M (data not shown). Since A β_{25-35} and full length A β_{1-42} cause neuron death by similar mechanisms (22), A β_{25-35} 50 μ M was used in all subsequent experiments.

FIG. 1. Neuroprotective effects of FBP on hippocampal organotypic slices culture

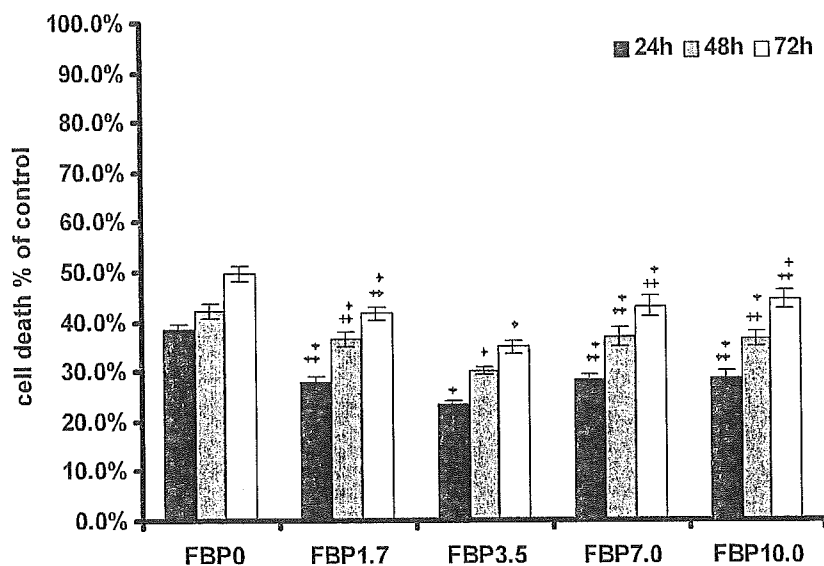


FIG. 1. Neuroprotective effects of FBP on hippocampal organotypic slices culture. Various concentration of FBP were added to the media. Compared with control group (FBP 0 mM, $n=36$), the addition of FBP significantly reduced the cell death in hippocampal slices at 24h, 48h and 72h after treatment. FBP 3.5mM has better neuroprotective effect than those of other FBP groups (each $n=42$). *:compare with FBP 0 mM group, $P<0.05$ + *:compare with FBP 3.5 mM group $P<0.01$.

Neuroprotective effect of FBP in hippocampal slices

Various concentration of FBP (0 mM, 1.7 mM, 3.5 mM, 7 mM, 10 mM) were added to the media. Compared with control group (FBP 0 mM), the addition of FBP significantly reduced the cell death in hippocampal slices at 24h, 48h and 72h after treatment (shown in FIG. 1). Interestingly, this neuroprotective effect of FBP was not in a dose-dependent manner. Compared with other FBP concentration groups, FBP 3.5 mM has better neuroprotective effect than those of other FBP groups (FBP 3.5mM group vs other FBP concentration groups, all the $P<0.01$).

Neuroprotective effect of FBP against A β induced neurotoxicity in hippocampal slices

As shown in FIG.2, treatment with FBP significantly decreased A β induced cell death in hippocampal slices at 24h, 48h and 72h (All the FBP concentration groups compare with control group, $P<0.01$). Similarly, this neuroprotective effect of FBP against A β was not in a dose-dependent manner. FBP 3.5mM group has better neuroprotective effect than that of other FBP concentration groups(FBP 3.5mM+A β group vs other FBP concentration groups, all the $P<0.01$)

Neuroprotective effect of FBP against A β induced neurotoxicity was attenuated by PLC, MEK or ERK inhibitors

Some other studies suggested that the neuroprotective action of FBP against hypoxia was dependent on PLC, MEK/ERK pathways, and this was also found to be the case with the hippocampal slices when exposure to A β induced neurotoxicity. Protective effect of FBP 3.5 mM against A β induced neurotoxicity in hippocampal slices was abolished by PLC inhibitor, U73122, MEK inhibitor, U0126, and ERK inhibitor, PD98059 at 24h, 48h and 72h. However, administration of chelerythrine, a protein kinase C inhibitor, did not modulate the neuroprotection of FBP against A β induced neurotoxicity in hippocampal slices (FIG. 3).

NEUROPROTECTIVE EFFECTS OF FBP AGAINST A β

FIG. 2. Neuroprotective effects of FBP against A β induced neurotoxicity on cultural hippocampal slices

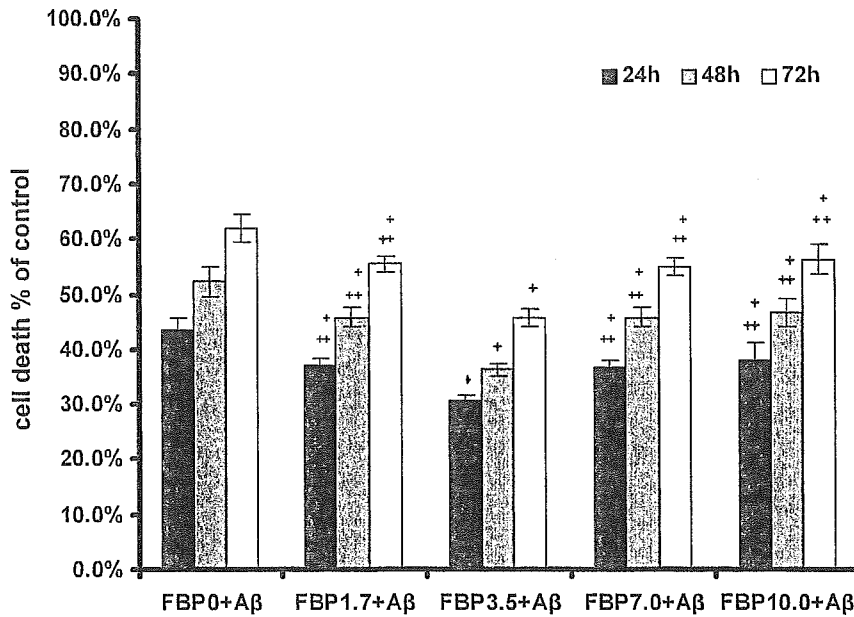


FIG. 2. Neuroprotective effects of FBP against A β induced neurotoxicity on cultural hippocampal slices. Treatment with FBP significantly decreased A β induced cell death in hippocampal slices at 24h, 48h and 72h. FBP 3.5mM group has better neuroprotective effect than those of other FBP concentration groups (each n=39). + : compare with control group (FBP 0 mM, n=36), P<0.01, ++ : compare with FBP 3.5 mM group, P<0.01.

FIG. 3. PLC inhibitor, MEK inhibitor, and ERK inhibitor attenuated the neuroprotective effect of FBP 3.5mM against A β induced neurotoxicity in hippocampal slices

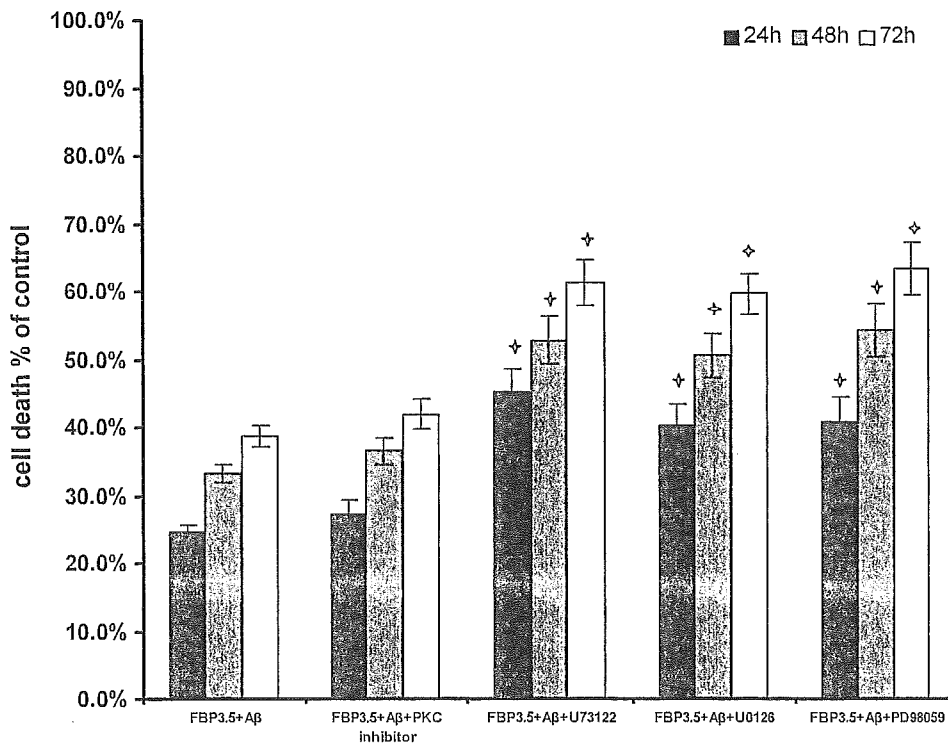


FIG. 3. Co-treatment with PLC inhibitor U73122 (n=45), MEK inhibitor U0126 (n=39), and ERK inhibitor PD98059 (n=48) attenuated the neuroprotective effect of FBP 3.5mM against A β induced neurotoxicity in hippocampal slices at 24h, 48h and 72h. Administration of chelerythrine, a protein kinase C inhibitor (n=36), did not modulate the neuroprotection of FBP 3.5 mM against A β induced neurotoxicity. + : compare with control group (FBP 3.5mM+A β , n=48), P<0.01.

FIG. 4. Effects of FBP on the ATP levels of hippocampal slices in the absence of $A\beta$

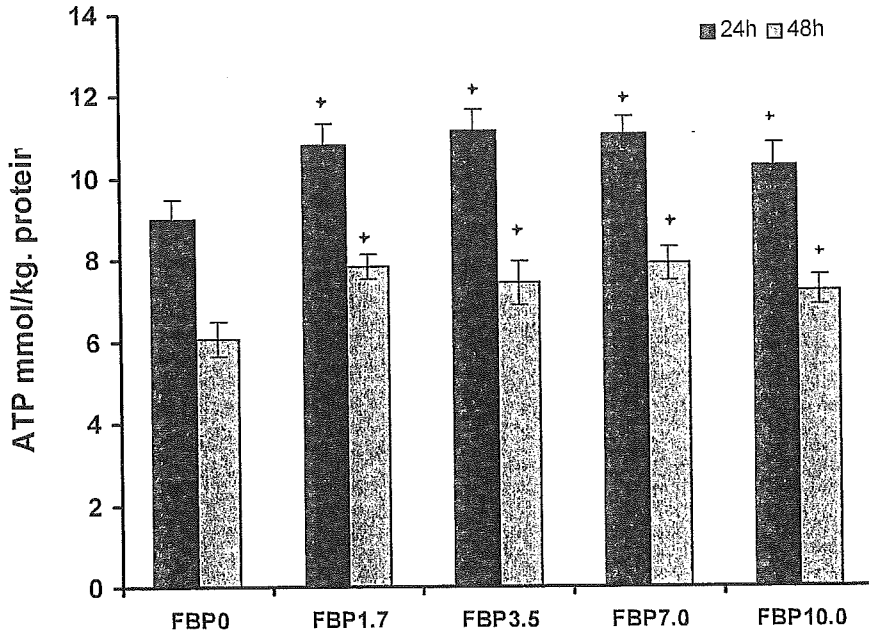


FIG. 4. Effects of FBP on the ATP levels of hippocampal slices in the absence of $A\beta$. Compared with control group (FBP 0 mM, n=48), FBP groups (concentration ranging from 1.7 mM to 10 mM, each n=36) had significant elevated ATP levels in the absence of $A\beta$ in hippocampal slices at 24h and 48h. However, the ATP levels were not significantly different among these FBP groups. + : Compare with control group (FBP 0mM), $P < 0.001$.

FIG. 5. Effects of FBP on the ATP levels of hippocampal slices in the presence of $A\beta$

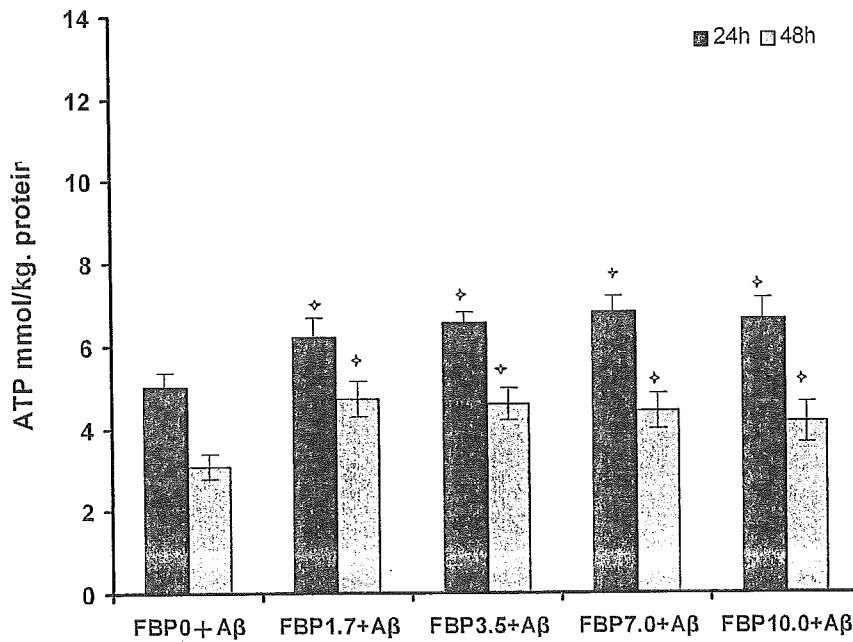


FIG. 5. Effects of FBP on the ATP levels of hippocampal slices in the presence of $A\beta$. The ATP levels were preserved at each concentration of FBP. However, the difference of the ATP levels among these various FBP concentration groups (each n=36) did not reach to significance. + : compare with FBP 0 + $A\beta$ group (n=36), all the $P < 0.001$.

NEUROPROTECTIVE EFFECTS OF FBP AGAINST A β

Effects of FBP on the ATP levels of hippocampal slices in the presence or absence of A β

To test the hypothesis whether the neuroprotective action of FBP against A β induced neurotoxicity was due to its role as an alternative energy source, we examined the effect of various concentrations of FBP on the ATP levels in hippocampal slices in the presence or absence of A β . Compared with control group (FBP 0mM), FBP groups (concentration ranging from 1.7 mM to 10 mM) had significant elevated ATP levels in hippocampal slices at 24h and 48h in the absence of A β (all the $P < 0.001$). The ATP levels were not significantly different among these FBP groups (FIG.4). With the presence of A β , the results were similar with those without A β , and the ATP levels were preserved at each concentration of FBP (compare with FBP 0 mM+A β group, all the $P < 0.001$). However, the difference of the ATP levels among these various FBP concentration groups did not reach to significance (FIG. 5).

Effects of PLC, MEK, ERK or PKC inhibitors on the ATP levels in hippocampal slices in the presence of FBP and A β

To investigate whether energy metabolism is involved in the neuroprotective action of FBP against A β toxicity through specific signaling pathways, ATP levels were examined when co-treated with specific inhibitors. Compared with control group (FBP 3.5 mM+A β), the addition of PLC inhibitor, MEK inhibitor, ERK inhibitor or PKC inhibitor did not cause significant difference in the ATP levels in hippocampal slices at 24h and 48h (FIG.6).

FIG. 6. Effects of PLC, MEK, ERK and PKC inhibitors on the ATP levels in hippocampal slices in the presence of FBP and A β

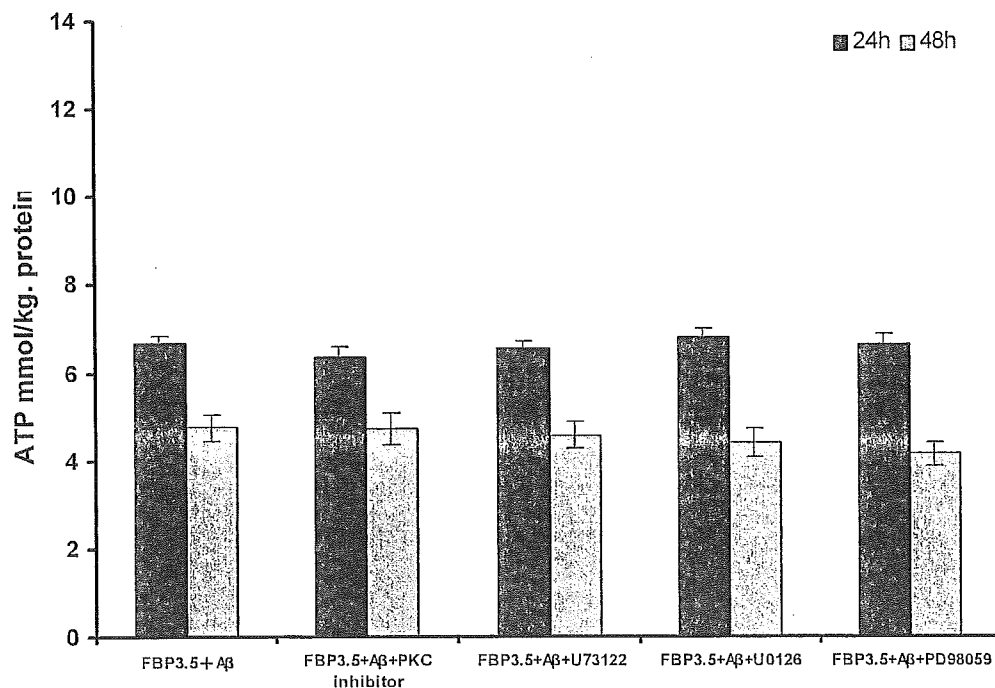


FIG. 6. Effects of PLC, MEK, ERK and PKC inhibitors on the ATP levels in hippocampal slices in the presence of FBP and A β . Co-treatment with PLC inhibitor (n=36), MEK inhibitor (n=36), ERK inhibitor or PKC inhibitor (n=36) did not cause significant difference in the ATP levels in hippocampal slices at 24h and 48h in the presence of FBP 3.5 mM and A β .

DISCUSSION

We have shown that exogenous FBP reduced A β induced cell toxicity in rat hippocampal slices. This neuroprotective effect of FBP might be the result of additional supply of ATP in the hippocampal slices. However, the neuroprotective action of FBP against A β induced neurotoxicity was not dose-dependent, and the ability of FBP to produce or preserve ATP was not dose-dependent, either. The results therefore suggests that protective action of FBP against A β induced neurotoxicity in hippocampal slices was due to, at least in part, other than its role as an alternative energy substrate to yield additional ATP. Furthermore, co-treatment of specific signaling pathways inhibitors with FBP and A β reduced the cell viability without alternating ATP levels, suggesting that protective action of FBP against A β induced neurotoxicity was not only due to its role as an alternative energy source, but also a modulator for neuroprotective signaling pathways.

FBP has been shown to attenuate tissue damage resulted from myocardial or kidney ischemia (7,4). Many studies demonstrated that FBP has neuroprotective effect in central nervous system against hypoxia/ischemia (30,31). Here we showed that FBP attenuated the neuron death induced by A β in hippocampal slices in a non dose-dependent manner, and also the ability of FBP to preserve the ATP levels appears not to be related to its concentrations. Because of its role as an intermediate products in glycolysis, it has been widely assumed that the protective effects of exogenous FBP results from its serving as an additional substrate for glycolysis (12). But our findings didn't seem to consist with this hypothesis since the increasing of FBP could not lead to the ATP elevation in a dose-dependent manner in hippocampal slices during A β exposure. To our knowledge, there are no specific transporters for FBP in the central nervous system. FBP is a highly negative charged molecular which is not easy to cross the hippocampal cellular membranes. Considering the fact that FBP was not taken up by red blood cell (26) or myocardial tissue (8), it was hypothesized the FBP would first have to undergo hydrolysis to fructose in order to be utilized. However some other experiments have demonstrated that, unlike FBP, addition of fructose or fructose-6-phosphate did not have neuroprotective effects (10). It seems that relatively small amounts of exogenous FBP could be metabolized by hippocampal slices.

While it seems only small amount of FBP could be uptaken by hippocampal culture cells, they are probably insufficient to explain its role as an energy substrate to maintain ATP level in hippocampal slice cultures. However, we could not exclude the possibility that this level of FBP might be sufficient to regulate energy metabolism and to modulate intracellular second messenger system. Some investigators illustrated that exogenous FBP has biphasic effects on the neuronal cellular metabolism. On one hand, FBP promotes glucose metabolism in astrocytes via pentose phosphate pathway (16). PPP is quite active in the CNS (35,17) and stimulation of PPP may lead to the increasing production of NADPH, synthesis of fatty acids, triglycerides, and phospholipids, then reduces oxygen radical injury of neural cell by regulating glutamine peroxidase (18,32). On the other hand, exogenous FBP may reduce the uptake of glucose from extracellular environment (16), and, moreover, it could inhibit the activity of phosphofructokinase (PFK)-the key enzyme of glycolysis, therefore reduce the production of lactate and the activity of TCA cycle (16). Our findings that neither higher nor lower levels of FBP cause better neuroprotective effects could be partially explained by this dual effects of FBP on the metabolism of neural cells.

Besides its role for serving as a metabolism regulator in the neuroprotective effects of FBP, the possible involvement of FBP in several intracellular signaling pathways should be taken into account. Recent studies have shown that neuroprotective qualities of FBP on

NEUROPROTECTIVE EFFECTS OF FBP AGAINST A β

hypoxia/ischemia- induced toxicity in hippocampal slices are dependent on PLC (5) and MEK/ERK pathways (6). In consistent with these studies, our observations also imply that PLC and ERK/MEK pathways are involved in the neuroprotective effects of FBP against A β induced neurotoxicity in hippocampal slices. Co-administration of PLC or ERK/MEK pathway inhibitors attenuate the neuroprotective action of FBP, but without affecting the ATP levels in hippocampal slices. Intracellular signaling pathways play crucial roles in regulating the cellular response and survival following insults by neurotoxins such as A β . Since little of exogenous FBP could enter neurons to serve as a signal, it was hypothesized that FBP might initiate its neuroprotective signaling at or near the cell surface. On the cell surface, FBP stimulate lipolysis (3) through PLC pathway and increase the production of diacylglycerol and inositol triphosphate, leading to the elevation of intracellular Ca²⁺. The consequence of this event is the activation of MEK/ERK signaling pathway and the expression of neuroprotective genes. Another important intracellular signaling system is PKC, a family of 12 serine/threonine kinase (23). Since PKC has been found to modulate cell viability resulting in the protection of various neuronal cells (27), we also investigated here if PKC pathway was involved in the neuroprotection of FBP. However, our data indicate that co-treatment of PKC inhibitor did not make significant alternations of both cell death and ATP levels in hippocampal slices in the presence of FBP and A β , suggesting that PKC signaling pathway may not be involved in the neuroprotective effects of FBP against A β induced neurotoxicity in hippocampal slices.

In the present study, we first report that FBP has neuroprotective effects against A β induced neurotoxicity in hippocampal slices. The preservation of ATP and the involvement of PLC and MEK/ERK signaling pathways could explain FBP's role as a modulator for both energy metabolism and intracellular signaling pathways. Even more, some recent studies have revealed that FBP has immunomodulatory (2) and anti-inflammatory properties (1,24) in modulating cellular function. The mechanism of FBP's neuroprotective effects seems to be multifactorial, and extensive studies are required to reveal its complex roles as a neuroprotectant.

ACKNOWLEDGEMENTS

This work was supported by a Research Grant from the Novartis Foundation for Gerontological Research and a Grant-in-Aid for Scientific Research (17500473) from Japan Society for the Promotion of Science. We deeply appreciate Dr. Sakaguchi, T., and Dr. Yang, B for technical assistance.

REFERENCES

1. **Alves, J.C., R.C. Santos, T.A. Castaman, and J.R. Oliveira.** 2004. Anti-inflammatory effects of fructose-1,6-bisphosphate on carrageenan-induced pleurisy in rat. *Pharmacol Res.* **49**:245-248.
2. **Bordignon, N.F., G.C. Meier, J.C. Alves, A. Lunardelli, E.Caberlon, A. Peres, and Rodrigues de Oliveira, J.** 2003. Immunomodulatory effect of fructose-1,6-bisphosphate on T-lymphocytes. *Int. Immunopharmacol.* **3**:267-272.
3. **Chlouverakis, C.** 1968. The lipolytic action of fructose-1,6-diphosphate. *Metabolism* **17**:708-716.
4. **Didlake, R., K.A. Kirchner, J. Lewin, J.D. Bower, and A.K. Markov.** 1989. Attenuation of ischemic renal injury with fructose 1,6-diphosphate. *J Surg Res. Sep;* **47** (3): 220-226.

5. **Donohoe, P.H., C.S. Fuhrman, P.E. Bickler, Z.S. Vexler, and G.A. Gregory.** 2001. Neuroprotection and intracellular Ca^{2+} modulation with fructose-1,6-bisphosphate during in vitro hypoxia–ischemia involves phospholipase C-dependent signaling. *Brain Res.* **917**: 158–166.
6. **Fahlman, C.S., P.E. Bickler, B. Sullivan, and G.A. Gregory.** 2002. Activation of the neuroprotective ERK signaling pathway by fructose-1,6-bisphosphate during hypoxia involves intracellular Ca^{2+} and phospholipase C. *Brain Res.* **958**:43-51.
7. **Fairas, L.A., M. Willis, and G.A. Gregory.** 1986. The effects of fructose 1-6 diphosphate glucose and saline on cardiac resuscitation. *Anesthesiology* **65**:595–601
8. **Galzigna, L., V. Rizzoli, M. Bianchi, M.P. Rigobello, and R. Scuri.** 1989. Some effects of fructose-1,6-diphosphate on rat myocardial tissue related to a membrane-stabilizing action. *Cell Biochem Funct.* **7**: 91-96.
9. **Gobbel, G.T., T.Y. Chan, G.A. Gregory, and P.H. Chan.** 1994. Response of cerebral endothelial cells to hypoxia: modification by fructose-1,6-bisphosphate but not glutamate receptor antagonists. *Brain Res.* **653**:23–30.
10. **Gregory, G.A., A.C. Yu, and P.H. Chan.** 1989. Fructose-1,6-bisphosphate protects astrocytes from hypoxia damage. *J. Cereb. Blood. Flow Metab.* **9**:29-34.
11. **Gregory, G.A., F.A. Welsh, A.C. Yu, and P.H. Chan.** 1990. Fructose-1,6-bisphosphate reduces ATP loss from hypoxic astrocytes. *Brain Res.* **516**:310-312.
12. **Hardin, C.D. and T.M. Roberts.** 1994. Metabolism of exogenously applied fructose 1,6-bisphosphate in hypoxic vascular smooth muscle. *Am. J. Physiol.* **267**:2325-2332.
13. **Hassinen, I.E., E.M. Nuutinen, K. Ito, S. Nioka, G. Lazzarino, B. Giardina, and B. Chance.** 1991. Mechanisms of the effect of exogenous fructose 1,6-bisphosphate on myocardial energy metabolism. *Circulation* **83**:584–593.
14. **Iwata, N., M. Higuchi, and T.C. Saido.** 2005. Metabolism of amyloid-beta peptide and Alzheimer's disease. *Pharmacol. Ther.* **18**, Epub ahead of print.
15. **Izumi, Y., A.M. Benz, H. Katsuki, M. Matsukawa, D.B. Clifford, and C.F. Zorumski.** 2003. Effects of fructose-1,6-bisphosphate on morphological and functional neuronal integrity in rat hippocampal slices during energy deprivation. *Neuroscience* **116**:465-475.
16. **Kelleher, J.A., P.H. Chan, T.Y. Chan, and G.A. Gregory.** 1995. Energy metabolism in hypoxic astrocytes: protective mechanism of fructose-1,6-bisphosphate. *Neurochem. Res.* **20**:785-792.
17. **Larrabee, M.G.** 1980. Metabolic disposition of glucose carbon by sensory ganglia of 15-day-old chicken embryos, with new dynamic models of carbohydrate metabolism. *J. Neurochem.* **35**:210-231.
18. **Lazzarino, G., A.R. Viola, L. Mulieri, G. Rotilio, and I. Mavelli.** 1987. Prevention by fructose-1,6-bisphosphate of cardiac oxidative damage induced in mice by subchronic doxorubicin treatment. *Cancer Res.* **47**:6511-6516.
19. **Liniger, R., R. Popovic, B. Sullivan, G.A. Gregory, and P.E. Bickler.** 2001. Effects of neuroprotective cocktails on hippocampal neuron death in an in vitro model of cerebral ischemia. *J Neurosurg Anesthesiol.* **13**:19-25.
20. **Macklis, J.D. and R.D. Madison.** 1990. Progressive incorporation of propidium iodide in cultured mouse neurons correlates with declining electrophysiological status: a fluorescence scale of membrane integrity. *J. Neurosci. Methods.* **31**:43-46.
21. **Markov, A.K., N. Oglethorpe, M. Grillis, W.A. Neely, and H.K. Hellems.** 1983. Therapeutic action of fructose-1,6-diphosphate in traumatic shock. *World J. Surg.* **7**:430–436.

NEUROPROTECTIVE EFFECTS OF FBP AGAINST A β

22. **Mattson, M.P.** 1997. Cellular actions of beta-amyloid precursor protein and its soluble and fibrillogenic derivatives. *Physiol. Rev.* **77**:1081-1132.
23. **Musashi, M., S. Ota, and N. Shiroshita.** 2000. The role of protein kinase C isoforms in cell proliferation and apoptosis. *Int. J. Hematol.* **72**:12-19.
24. **Nunes, F.B., C.M. Graziottin, F.J. Alves, A. Lunardelli, M.G. Pires, P.H. Wachter, and J.R. Oliveira.** 2003. An assessment of fructose-1,6-bisphosphate as an antimicrobial and anti-inflammatory agent in sepsis. *Pharmacol. Res.* **47**:35-41.
25. **Okada, Y.** 1974. Recovery of neuronal activity and high-energy compound level after complete and prolonged brain ischemia. *Brain Res.* **72**:346-349.
26. **Rigobello, M.P., M. Bianchi, and R. D. Galzigna.** 1982. Interaction of fructose-1,6-bisphosphate with some cell membranes. *Agressologie* **23**:63-66.
27. **Saito, N. and Y. Shirai.** 2002. Protein kinase C gamma (PKC gamma): function of neuron specific isotype. *J. Biochem.* **132**: 683-687.
28. **Sakaguchi, T., M. Okada, and K. Kawasaki.** 1994. Sprouting of CA3 pyramidal neurons to the dentate gyrus in rat hippocampal organotypic cultures. *Neurosci. Res.* **20**:157-164.
29. **Sakurai, T., B. Yang, T. Takata, and K. Yokono.** 2002. Synaptic adaptation to repeated hypoglycemia depends on the utilization of monocarboxylates in uinea pig hippocampal slices. *Diabetes* **51**:430-438.
30. **Sola, A., M. Berrios, R.A. Sheldon, D.M. Ferriero, and G.A. Gregory.** 1996. Fructose-1,6-bisphosphate after hypoxic ischemic injury is protective to the neonatal rat brain. *Brain Res.* **741**: 294-299.
31. **Takata, T., M. Nabetani, and Y. Okada.** 1997. Effects of hypothermia on the neuronal activity, [Ca²⁺] accumulation and ATP levels during oxygen and/or glucose deprivation in hippocampal slices of guinea pigs. *Neurosci. Lett.* **227**:41-44.
32. **Tavazzi, B., L. Cerroni, D. D. Pierro, G. Lazzarino, M. Nuutinen, J.W. Starnes, and B. Giardina.** 1990. Oxygen radical injury and loss of high-energy compounds in anoxic and reperfused rat heart: prevention by exogenous fructose-1,6-bisphosphate. *Free Radic Res. Commun.* **10**:167-176.
33. **Yanagisawa, K.** 2000. Neuronal death in Alzheimer's disease. *Int. Med.* **39**: 328-330.
34. **Zhang, J.N., F.M. Zhang, W.S. Ma, and T. Forrester.** 1988. Protective effect of exogenous fructose-1,6-diphosphate in cardiogenic shock. *Cardiovasc. Res.* **22**:927-932.
35. **Zubairu, S., J.S. Hothersall, A.E. Hassan, P. McLean, and A.L. Greenbaum.** 1983. Alternative pathways of glucose utilization in brain: changes in the pattern of glucose utilization and of the response of the pentose phosphate pathway to 5-hydroxytryptamine during aging. *J. Neurochem.* **4**:76-83.